JOURNAL OF VIROLOGY, June 1974, p. 1176-1185

Vol. 13, No. 6
Printed in U.S.A.

Locating Interrupted Hydrogen Bonding in the Secondary Structure of PM2 Circular DNA by Comparative Denaturation Mapping

R. J. JACOB,[1] J. LEBOWITZ, AND A. K. KLEINSCHMIDT[2]

Department of Biology, Syracuse University, Syracuse, New York 13210, and Department of Biochemistry, New York University School of Medicine, New York, New York 10016

Received for publication 14 January 1974

Previous studies with HCHO have revealed a reaction with superhelical DNA that strongly suggests that this DNA consists of small regions of interrupted secondary structure. To map these sites in PM2 DNA, the following set of experiments was performed using electron microscopy. (i) A denaturation map of nicked form II was obtained using Inman's alkaline-HCHO conditions. (ii) The superhelical form I was reacted with HCHO at 30 C until equilibrium was achieved at the interrupted sites (3.6% reactivity). The excess HCHO was removed rapidly and X-ray treatment was employed to nick these prereacted molecules. These form II molecules containing HCHO (form II HCHO) were also subjected to denaturation mapping. It would be expected that the HCHO-unpaired regions would serve as induction sites for the propagation of melting. Hence, depending on the location of the induction sites, we would anticipate either the creation of new regions of melting or a normal denaturation map shifted to lower pH values. Comparison of the development of progressive denaturation of form II and form II HCHO reveals that the latter is the case. The denaturation maps of form II are highly organized patterns of adenine-thymine (AT)-rich regions, with a total of five regions at extreme pH conditions. There are six highly organized regions for form II HCHO, i.e., smaller adjacent loops, at low denaturation conditions where no denaturation is seen for form II. These coalesce into the pattern for form II containing four of five A-T-rich regions observed for form II. Hence we conclude that the regions of altered hydrogen bonding in superhelical PM2 DNA are four to six in number and they map in the A-T-rich regions of the DNA.

The characterization of the secondary structure of superhelical DNA (form I) has led to the discovery that it contains alterations or interruptions in the duplex structure that are not present in open nicked circular form (form II) of these DNAs (5). Studies of the reactivity of formaldehyde (HCHO) (5), methylmercuric hydroxide (3), and the activities of single-strand-specific endonucleases (2, 13) have all led to the same interpretation, i.e., that the supercoiled form I of ϕX-RF and PM2 DNAs, as well as SV40 DNA, contains a significant number of unpaired or weakly paired bases. Hydrogen-tritium exchange and the detailed kinetic analysis of the HCHO reaction with PM2 DNA (R. J. Jacob, J. Lebowitz, and M. Printz, Nucleic Acids Res., in press) have shown that such reactions are not due to a difference in the breathing rates of form I when compared to the form II molecule, but due to a localized region(s) that represents approximately 3.5% of the total helix (3, 5). In the case of SV40 DNA I, it has been concluded that at least two regions exist which are sensitive to the action of S1 endonuclease (2). This work came to our attention considerably after the initiation of this study.

When the altered secondary structure of PM2 DNA I was fully reacted with HCHO and the molecule was examined by electron microscopy, using aqueous spreading conditions that unwind supercoils, no detectable denatured region(s) could be visualized. No firm conclusion could be reached from this preliminary attempt to locate "single-strand-like region(s)" except that it was unlikely that the total altered secondary structure was located in one site on the superhelical molecule. Therefore, our approach shifted to the hypothesis that PM2 DNA

[1] Present address: University of Chicago, Department of Microbiology, Chicago, Ill. 60637.
[2] Present address: University of Ulm, Ulm, West Germany.

I contains several partially disordered regions and that it would be again unlikely that we could locate these sites without amplification of the denaturation process through further HCHO-assisted melting (14). However, in the case of superhelical DNA a unique situation prevails; any base that reacts with HCHO is a potential defect that would be retained if form I HCHO is converted to form II HCHO by a strand scission. Hence, these formylated bases would now function as nucleation sites for the further denaturation of duplex structure propagating from the defects. A theoretical kinetic treatment for the HCHO-assisted unwinding at defects has been shown to be in agreement with the experimental data of sedimentation analysis and electron microscopy (1, 15). Hence, we can expect propagation to occur at the formylated altered sites when such a molecule is nicked and subjected to further melting. Moreover, these induction sites can be compared to the normal low melting nucleation sites (adenine-thymine [A-T]-rich sequences) controlled by the primary structure as found in untreated form II DNA (10-12). This comparative analysis should allow us to observe a denaturation map for form I HCHO at lower pH treatments than those needed for form II or a more advanced profile at identical pH incubations. From this data it should be possible to answer the following questions regarding superhelical DNA. Is the altered region(s) (defects) located solely in the A-T-rich sequences or is another denaturation pattern generated that indicates different map positions for these sites? Can we obtain a reasonable estimate of the number of nucleation sites from this data? To our best knowledge this is the first attempt to use denaturation mapping by electron microscopy to locate preexisting defects in DNA secondary structure by taking advantage of the different reactivities imposed by structural variations.

MATERIALS AND METHODS

Virus growth and purification. The bacteriophage PM2 and its host *Pseudomonas* bal-31 was grown and purified as described previously (6). The only modification made was the use of a 5 to 20% sucrose (1.0 M NaCl, 0.02 M Tris, pH 8.1) gradient, centrifuged in an SW27 rotor at 20,000 rpm, 10 C, for 40 min rather than isopycnic centrifugation for phage purification.

Extraction and purification of the DNA. The DNA was extracted from the PM2 phage by phenol and purified, as described previously (7), with the modification that extraction of ethidium bromide (ETHBr), after CsCl-ETHBr isopycnic centrifugation, was with isoamyl alcohol. The DNA was characterized by analytical centrifugation (sedimentation and buoyant density analysis) in a Beckman model E ultracentrifuge equipped with a multiplexer and photoelectric scanner. Preparations of the superhelical circular form I DNA contained 5 to 15% open circular form II DNA, and this was confirmed by microscopy. Sedimentation analysis in alkaline CsCl showed that most of this form II was single nicked molecules. The DNA was stored frozen at −35 C after dialysis into BB buffer (0.01 M sodium borate, 0.15 M NaCl, pH 9.0).

Preparation of form I HCHO (formaldehyde-equilibrium) material. Form I DNA that has reacted with formaldehyde until equilibrium is referred to as form I HCHO material. This was prepared by reacting 1 absorbance unit at 260 nm (A_{260}) (50 μg/ml) of form I DNA in BB buffer with 1.3 M HCHO for 3 h at 30 C. Under these conditions no detectable reaction is observed for form II. The HCHO was prepared as described (5) to eliminate polymeric paraformaldehyde. All HCHO concentrations were determined by the chromotropic acid spectral procedure (4). The preparation of form I HCHO was monitored spectrophotometrically by the Cary 16 UV-Vis spectrophotometer coupled to a Lauda K-2/R constant-temperature unit. The 3-h reaction would give a final hyperchromicity of approximately 0.021 at 270 nm.

Conversion of form I HCHO to form II HCHO by X irradiation. Form I HCHO was passed through a Sephadex column (10 by 1 cm) equilibrated with BB buffer at 27 C immediately after the HCHO reaction was completed. The appropriate fractions containing form I HCHO were collected. This procedure is similar to that technique used in tritium-hydrogen exchange (16). Free HCHO was removed since X irradiation in the presence of 1.3 M HCHO required abnormally high doses to convert form I HCHO to form II HCHO, due most likely to a quenching process. The removal of HCHO also insures against the propagation of denaturation in the successive steps before controlled pH melting. The DNA form I HCHO was frozen and kept at −35 C or at lower temperatures. Samples of freshly-thawed form I HCHO (0.1 ml of each DNA, 50 to 60 μg/ml in BB buffer) was X-irradiated with 1,000 rads (less than 2 min irradiated at 0 C) using a Picker-Vanguard X-ray therapy generator, 280 kV, HVR 1.3 mm Cu, to convert about 65% of the form I HCHO to form II HCHO (formaldehyde-equilibrium form II). This conversion was considered best for denaturation mapping since higher doses of X rays would produce a population of multiply-nicked form II HCHO molecules that could fragment upon denaturation mapping.

Partial denaturation of DNA by alkaline formaldehyde. Form I and II, form I HCHO, and form II HCHO material, prepared as described above and stored frozen (−35 C or colder), were thawed immediately before use. Each preparation was controlled using small portions of thawed material in our standard protein monolayer technique to verify size and configuration (see Materials and Methods).

Open circular DNA (form II or form II HCHO in borate buffer) was prepared for denaturation mapping by the partial denaturation techniques described by Inman (Methods in enzymology, in press). Partial strand separation is obtained by reacting relaxed

DNA with alkaline formaldehyde (3.2 M final concentration and 0.06 M Na^+) (12). A 10-μliter sample of DNA (approximately 60 μg/ml, BB buffer) and 10 μliters of the alkaline formaldehyde were mixed and allowed to react for various periods between 2 and 10 min at 25.0 C. Each partial denaturation experiment was piloted by measuring the pH between 10.00 and 11.00 to two decimal values with a DNA-free mixture of the solution described above.

The reproducibility of repeated denaturation patterns (see Results) indicates strongly that the pH of the DNA solution mixture was retained at the value of the pilot solution and that no significant changes in pH occurred during the reaction period to influence the consistently observed melting profiles.

DNA-cytochrome c films. The alkaline formaldehyde reaction (20 μliters in volume) was stopped at various time intervals (see Results) by adding ice-cold solutions of 20 μliters of 0.1 M acetic acid, 140 μliters of M ammonium acetate, and 20 μliters of cytochrome *c* (1 mg/ml) to make a 0.2 ml spreading solution (14). This spreading solution, containing 2 to 3 μg of PM2 DNA per ml in 0.8 to 1 M ammonium acetate and 100 μg of cytochrome *c* per ml at pH 5.0 to 5.2, was not only used for alkaline formaldehyde-reacted material (form II and II HCHO) but also, as a control, for unreacted forms I, I HCHO, and forms II, II HCHO. After 2 min, the spreading solution was completed, and 0.1 ml was spread, over the clean surface of a 0.3 M ammonium acetate solution adjusted to pH 5.5 by acetic acid, in a Teflon-coated aluminum trough (300 cm^2 substrate area available). The DNA-cytochrome *c* film boundaries, indicated by a few talcum particles, achieved a maximum of film area (at least 1 m^2/mg of cytochrome *c*) very reproducibly.

Electron microscopy of DNA. The DNA-cytochrome *c* film was immediately transferred to carbon-collodion-coated platinum (Siemens type) grids by surface contact and stained with uranyl acetate in acetone (9). After "puffing" the collodion layer (in an air-pressured oven at 180 C, 10 min), the specimens were micrographed in bright-field and dark-field modes (using a magnetic tilt lens) of an Elmiskop IA electron microscopy, at 80 or 100 kV and operational magnification between 5,000 and 15,000 times. As magnification standards, cross-line grating replicas (2,610 lines/mm, E. Fullam, Inc.) were used.

Denaturation mapping of partially strand separated DNA. The micrographs (negatives) were rear-projected to a computerized coordinate system (RAND tablet, Grafacon 1010A board) interphased to a PDP-8 digital computer. Most of the molecules were measurable and traced with a hand stylus as fully extended circular form II type molecules; linear form III and entangled DNA were neglected. Denaturation sites or loops showing single-strand ends (broken loops) were rarely found and excluded from measurements.

Denaturation sites in PM2 DNA as linear representation of the electron microscope image were drawn from normalized lengths (see Results), and normalized standard deviation (±SD) in histograms and maps used throughout. In order to align properly the normalized maps of a collection of identical, partially denatured molecules, linear maps with denatured regions (rectangles, see Fig. 2) were aligned for maximum overlap by plotting each circular length as a fully redundant or single repetitious straight line, i.e., twice their unit length on paper strips (scaled to 5 cm = 1 μm). All molecules were then aligned on one side of a denatured (usually most prominent) region that was considered the first region appearing in the maps of minimally treated form II by alkaline formaldehyde. The stripped linear maps were then sectioned at a common point into unit length (see Results, Fig. 2) containing all the denaturation sites located at fractional length of the linear map. From linear maps, circular maps (see Fig. 4 and 7) were constructed accordingly.

RESULTS

Alkaline formaldehyde denaturation of form II. The histograms of the HCHO-alkaline pH denaturation of PM2 form II (Fig. 2, 3) were obtained from a compilation of micrographs of the type shown in Fig. 1.

It must be remembered that the histograms represent a summation of all the patterns observed at a particular denaturation constraint. Figure 2 illustrates this point by showing the alkaline HCHO reaction with form II at pH 10.97 for 3 min. The pattern of denaturation of a collection of molecules with more than one denaturation site falls into sets of molecules when the alignment procedure described in Materials and Methods (8) is employed. The most prominent denaturation site is designated loop A, and this is aligned to the left third of each molecule and an artificial origin is created 0.8 μm from the right side of this loop. Representative sets of molecules containing two and three loops can be seen in Fig. 2a. The histogram shown in Fig. 2b is the summation of all the sets of denatured molecules. Undenatured measurable molecules were also present on the micrographs (41%) and excluded from Fig. 2.

Figure 3 illustrates the progressive denaturation of form II in the form of histograms (Fig. 3a to d) at the indicated denaturation constraint. The histogram of Fig. 2b is repeated for clarity as Fig. 3b. The HCHO-alkali-induced denaturation constraint of pH 10.94 at 7 min was the lowest denaturation constraint to reveal a pattern for form II DNA. The histogram in Fig. 3a represents the frequency of denatured regions, loops A and B at 0.75 μm and 1.0 μm, respectively. This population also consisted of 41% single looped patterns (see Table 1).

The histogram for the data at pH 10.97 and 3 min reveals the appearance of a new loop C at 2.4 μm from the origin (Fig. 3b). The frequency of loop B increases at the denaturation constraint of pH 10.97 at 7 min and new loops emerge in low frequency between loops B and C (Fig. 3c).

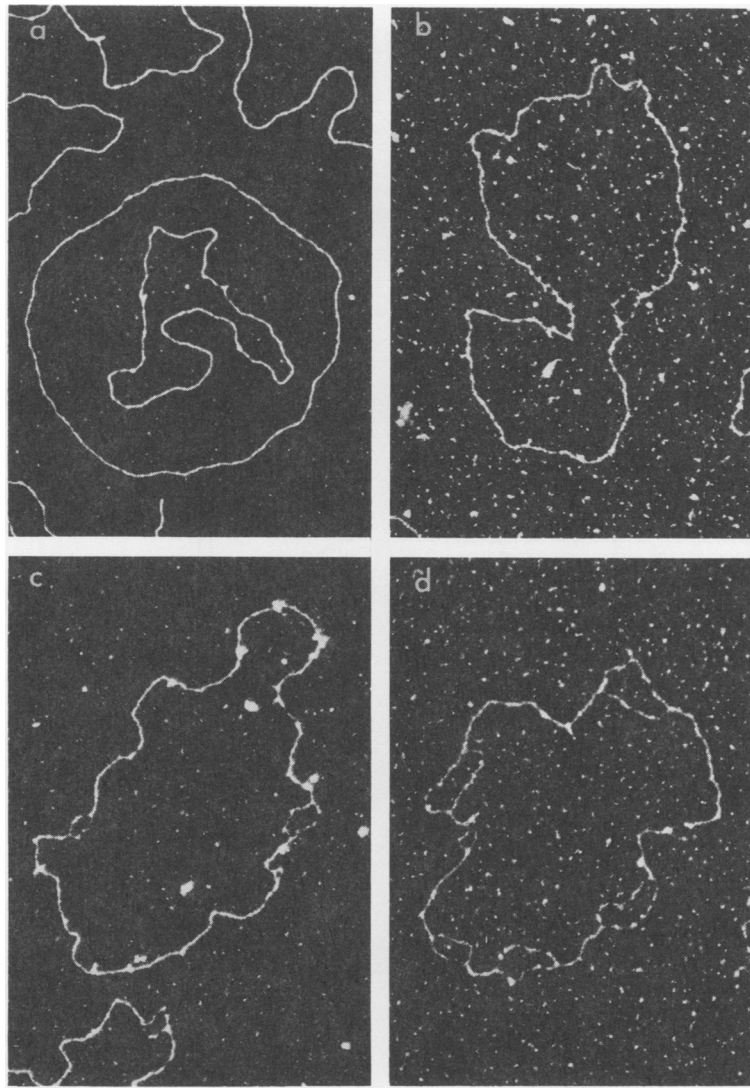

FIG. 1. *Electron micrographs of PM2 form II DNA (a) (×59,000) and patterns seen when this DNA was treated at various denaturation constraints. The DNA was treated, spread, and photographed. Form II DNA was seen as the different patterns described in Fig. 3 and 4. (b) Pattern 1 at pH 10.97 and 3 min (×59,000). (c) Pattern 2b at pH 10.97 and 7 min (×73,000). (d) Pattern 5 (a multiple-looped pattern) at pH 11.00 and 7 min (×73,000).*

The results of the most advanced treatment constraint of pH 11.0 at 7 min is represented by Fig. 3d. The frequency of loops A and B are about equal, and this most advanced pattern shows new loops D and E at 1.35 μm and 0.3 μm from the origin, respectively, to be approximately equal in frequency with loop C. This histogram has a lower number of molecules representing the population because of our restriction of measuring only molecules that did not contain single strand ends. At this advanced pattern such molecules are hard to find.

Denaturation patterns seen as an advancing profile. The linear maps of Fig. 2 and the histograms of Fig. 3 reveal an organization of patterns each within a particular denaturation constraint. It is useful and revealing to reconstruct simplified circular maps, each based on the assigned number of prominent loops present and their normalized locations on the maps. The circular maps are collected from within one experiment as indicated in Fig. 4. The "background" of denaturation (Fig. 2) is omitted. Each pattern is represented with the size for the

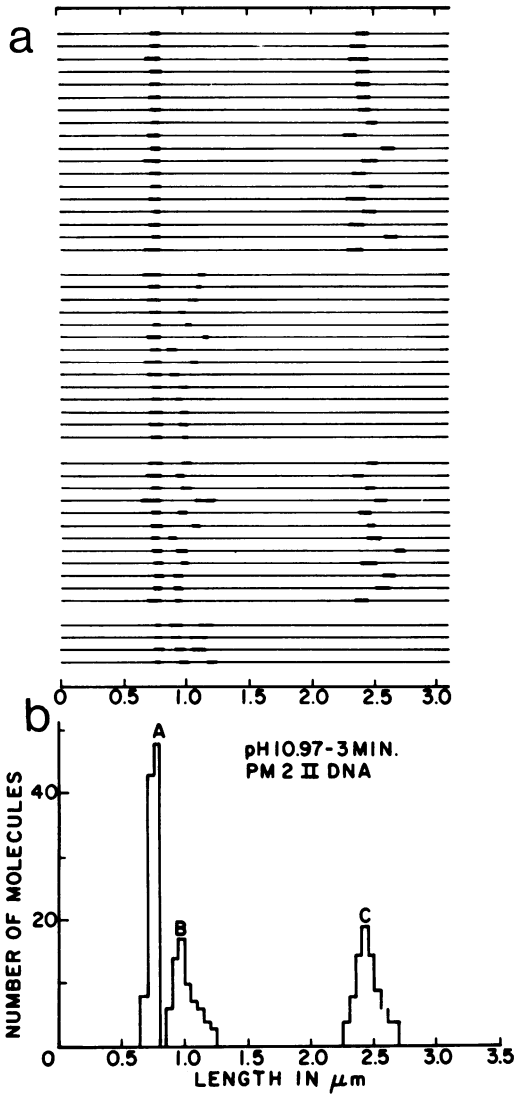

FIG. 2. *Denaturation map (a) accompanied by its respective histogram (b) showing the position and frequency of denatured sites for PM2 form II DNA molecules after partial denaturation at pH 10.97 and 3 min. The DNA was treated and measured, and the normalized lengths were plotted as linear molecules. Regions A, B, and C indicate denatured sites of increased frequency.*

region and its respective standard deviation. The letter after a loop represents the same loop as is assigned to the histograms. It can be easily determined by comparing the measurements of the patterns that pattern 3b is a composite of pattern 2a and 2b (Fig. 4a). As denaturation constraints increase, pattern 1 in the collection of DNA within one experiment diminishes and

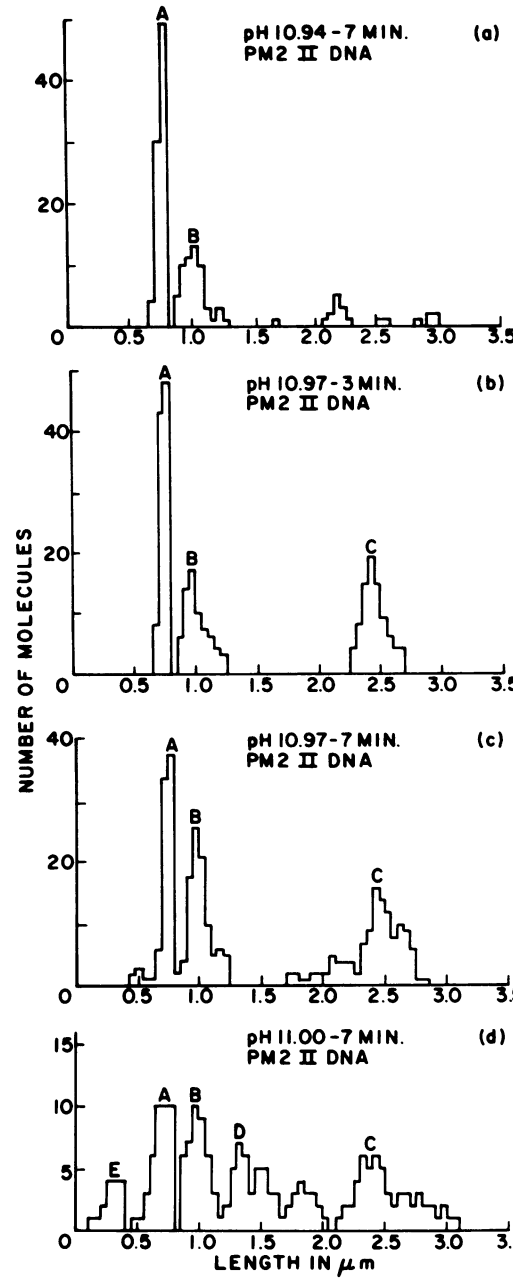

FIG. 3. *Histograms showing the position and frequency of denatured sites for PM2 form II DNA molecules after partial denaturation at (a) pH 10.94 and 7 min, (b) pH 10.97 and 3 min, (c) pH 10.97 and 7 min, and (d) pH 11.00 and 7 min. The DNA was treated and measured, and the normalized lengths were plotted as linear molecules. Regions A to E indicate denaturation sites and their particular frequency within the population. Loop A is considered the earliest region to titrate under the HCHO alkali denaturation constraints.*

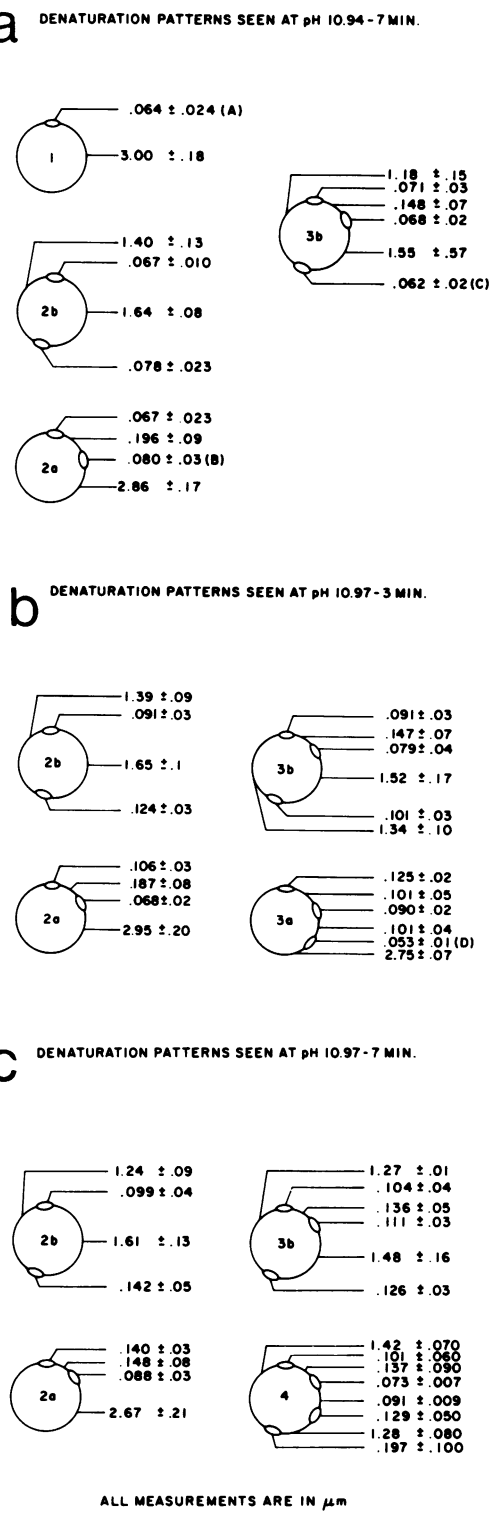

FIG. 4. *The schema of various patterns seen when PM2 II DNA was treated at the denaturation constraint of (a) pH 10.94 and 7 min, (b) pH 10.97 and 3 min, and (c) pH 10.97 and 7 min. The number-letter designations within the simple circular diagrams indicate the various patterns seen ("a" indicates adjacent loops; "b" indicates opposing loops). The looped regions are placed relative to each other with the size measurements and respective standard deviation recorded in micrometers. The letters in parenthesis after these measurements are loop designations that correspond to the denatured regions seen in the respective histograms. The solid lines are native regions with their appropriate measurements recorded. Electron micrographs of these patterns are seen in Fig. 1. It is obvious that the designation of the loop in the one-looped pattern 1 as loop A is arbitrary and its population could be representative of small populations of loops B and C. Pattern 3a is shown only in Fig. 4b since it has a minor frequency at both constraints. Pattern 5 is not shown since this is a multiple-looped pattern of five or more loops.*

the frequency of the advanced pattern 4 increases. Pattern 4 is generated from 3b which is the predominant three-loop circle (Table 1). However, the former pattern could also be generated from the low-frequency pattern 3a (Table 1). This latter pattern appears to be made up of loops A, B, and D from the skewness observed in the histograms for the B loop (Fig. 2b).

The occurrence in the populations of patterns 1 to 4 are represented in the first four columns of Table 1. The pattern 5 reported (bottom line) in the table is a pattern that is too advanced (with increasing number and higher percentage of denaturation sites) to be simply organized and represents a multiple-looped (five or more loops) pattern with greater fluctuation (Fig. 3d) than is seen in the less advanced patterns. The constraint of pH 11.00, 7 min, was represented by a smaller number of molecules, which was considered to be insufficient data to be represented as an organization of simple circular maps. These columns in Table 1, when compared with the corresponding histograms and maps of Fig. 3 and 4, show the advancing titration of the loops A to E, which reflect a virtual decrease in adenine-thymine richness (12) for this order. The reader is again referred to Fig. 1 for the electron micrographs of some of these patterns.

Denaturation maps of formaldehyde equilibrium material. It would be anticipated that denaturation loops in form II HCHO would propagate from the regions of unpaired bases that reacted with HCHO in form I. Therefore, it is now possible to compare the histograms of form II HCHO relative to our previous data for untreated form II.

Figure 5 shows the histograms of an experi-

TABLE 1. *Percentage of DNA molecules found in the patterns shown in Fig. 3, 4, and 5*

Pattern	Form II				Form II HCHO		Control form II
	10.94[a]	10.97	10.97	11.00	10.75	10.94	10.94
	7[b]	3	7	7	7	7	7
1	41[c]	0	0	0	0	0	26
2a	31	28	13	0	9	8	44
2b	12	40	13	0	0	0	13
3a	6	8	0	0	4	4	4
3b	10	24	52	20	9	15	13
4	0	0	10	20	26	24	0
5[d]	0	0	12	60	52	49	0

[a] pH value of denaturation constraint.
[b] Minute of denaturation constraint.
[c] Percent of the total population (DNA molecules) seen at that denaturation constraint.
[d] Pattern 5 is a multiple-looped pattern of five or more loops.

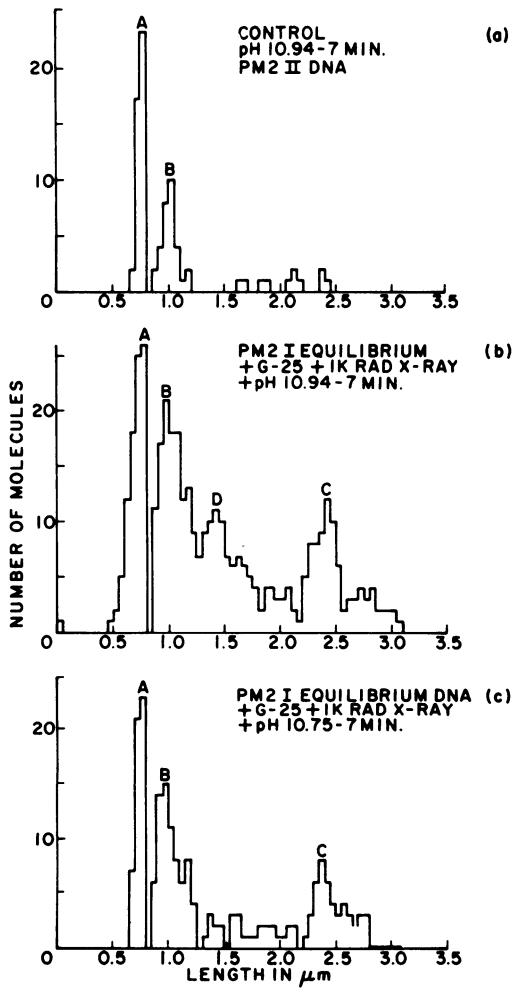

FIG. 5. *Histogram showing the position and frequency of denatured sites for PM2 form II HCHO DNA after partial denaturation at (b) pH 10.94 and 7 min and (c) pH 10.75 and 7 min. Fig. 5a is the control molecule PM2 form II DNA at pH 10.94 and 7 min. The form II HCHO DNA was prepared from form I HCHO DNA. All measurements and the treatment of data were as described for earlier histograms.*

ment with form II HCHO that has been obtained from form I HCHO by X-ray scission followed by alkaline formaldehyde reaction (Materials and Methods). Since pH 10.94, 7 min, was the lowest constraint to produce a pattern on form II, this was the first treatment applied to the form II HCHO material (Fig. 5b). When compared to the control experiment without formaldehyde pretreatment (Fig. 5a), this material gives a far more advanced pattern, which is similar to the one of form II treated at pH 11.00, 7 min (Fig. 3d). The main difference is the absence of loop E. However, the regions B, C, and D seem to be relatively more denatured in Fig. 3d than in Fig. 5b as can be seen by comparison with region A in both figures. This is probably the reason for the absence of E in Fig. 5b since less denaturation has taken place.

The location of these formaldehyde-equilibrium sites in form II HCHO coincides with the location of main denaturation sites seen in the native form II as loops A to D (Fig. 3). Since no pattern was observed for form II below pH 10.94, 7 min, the pattern for form II HCHO should begin at a significantly lower pH constraint.

Figure 5c confirms this prediction and shows that form II HCHO, when treated at pH 10.75, 7 min, gives rise to a three-loop pattern close to that found at pH 10.97, 7 min, with form II. The last three columns of Table 1 show the patterns and their percentage of occurrence within the population of these two DNA samples when

treated by the various denaturation constraints. No control experiment was recorded for pH 10.75, 7 min, for form II since no denaturation patterns were obtained. It should be emphasized again that form II HCHO DNA gives more advanced denaturation profiles, such as pattern 5 in Table 1, when compared to the lowest constraint showing denaturation for form II—pH 10.94, 7 min. Hence, of necessity, this had to be our control. With alkaline formaldehyde denaturation of form II HCHO, pattern 5 is the predominant pattern and, as a multiple-looped pattern seen for form II HCHO, is different in detail than that obtained for form II. Electron micrographs of these molecules show some of these patterns in Fig. 6. The multiple loops seen in this material contain an organization of adjacent loops which can be placed within one or more of the A-T-rich larger loops seen in the patterns of the higher constraints. In other words, we observe fine detail in these molecules in the sense that we can observe small adjacent loops that must coalesce to form the larger A and B loops as well as loop

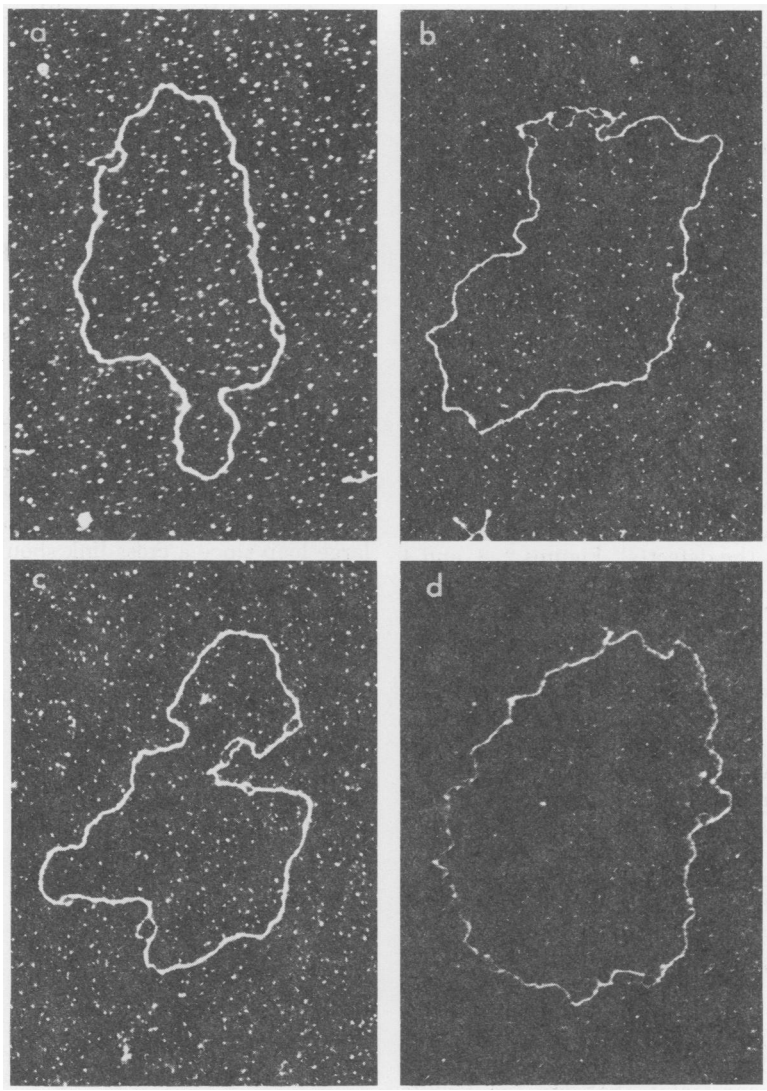

FIG. 6. *Electron micrographs of PM2 form II HCHO DNA and the patterns seen when this DNA was treated at the denaturation constraints indicated. The DNA was prepared, heated, spread and photographed. Typical advanced patterns seen at pH 10.75 and 7 min (a and d), and at pH 10.75 and 10 min (b and c), clearly localizing the induction sites into regions A to D. Fig. 6d at pH 10.75 and 7 min shows the double induction sites or regions A to C.* ×75,000.

C at lower frequency. A comparison of Table 1 with Fig. 5 reveals that pattern 5 is the predominant class of denatured molecules with five or more loops mapping at positions A, B, C, or D. However, these molecules are not advanced with regard to loop size but only to loop number, and it appears that we have succeeded in trapping precursors of the more advanced form II patterns (Fig. 1d).

Another possibility for the multiple loops could be an HCHO-mediated cross-linking that may occur during the prior incubation with HCHO. This could be an alternative mechanism for the observed fine structure.

With the above considerations it can be definitely concluded that form II HCHO shows a denaturation map of five or more loops which coalesce, and these map with the normal A-T-rich regions of form II. The advance nature of the profiles at lower constraints supports the concept of propagation of denaturation at defects. This data will be interpreted in Discussion in regard to the questions raised earlier about the location and number of altered regions in the superhelical form of PM2 DNA.

DISCUSSION

This is the first attempt to use comparative denaturation mapping of DNA to locate a defect or defects in a DNA duplex. The hydroxymethylated altered structure of PM2 form I DNA has been used as induction site(s) for subsequent denaturation-induced constraints in order to study the defect(s). Figures 2, 3, and 4 clearly show an advancing pattern for the denaturation of form II with three definite A-T-rich regions (A, B, and C) and a fourth (D) which is probably high in A-T content. The appearance of loop E is indicated at the pH 10.97 and 7 min constraint (Fig. 3c) at low frequency. However, its increase in accompanied by loops between D and C which we have not assigned letters (Fig. 3c and d). Hence, we can not conclude that this phase of denaturation is associated with low melting A-T sites. When form I HCHO DNA is freed of excess HCHO, converted to form II HCHO DNA by X rays, and denatured at lower constraints, we also observe denatured loops A to D mapping at the same positions that we obtained for form II. Therefore, we conclude that the regions of altered secondary structure are located in the A-T-rich regions and these sites served to promote advanced patterns at a denaturation constraint that are too low to produce any visible melting of form II molecules (Table 1, Fig. 6).

The pictures shown in Fig. 6 for the pH 10.75 and 7 min (Fig. 6d) constraint reveal that this earlier titration (lowest constraint) of the form II HCHO DNA is different than that seen for the lowest constraint to give a pattern on form II DNA. The A-T-rich loops A and B appear to titrate at two points within a region which is later seen (higher pH constraints) as a completely titrated region. This is not observed for the less A-T-rich D loop induction site present in form II HCHO. Some evidence exists for such double induction sites for region C, but this occurs at low frequency. This event would then place the number of independent induction sites at six, with four of these sites located proximally within the A and B regions. This is diagrammed in Fig. 7. These two sites would then coalesce to form one region as the denaturation constraints are increased in the treatment of form II HCHO. This effect cannot be seen on the histograms at pH 10.75 and 7 min (Fig. 5c), because the location of these adjacent induction sites within these regions does not seem to be unique. The fact that there are two induction sites in regions A and B would make them more susceptible to the denaturation constraints than region D, and this could explain the virtual absence of region D in the histogram of the lowest constraint, pH 10.75 and 7 min (Fig. 5c).

Again, we must temper the above discussion of multiple loops with the possibility that they are simply due to cross-links. However it is difficult to understand the mechanism of the conversion of two adjacent multiple loops into a large loop since a cross-link should be a stable methylene bridge (8).

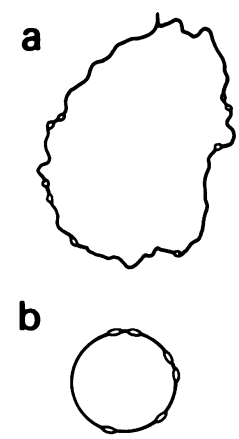

FIG. 7. *(a) Schematic representation of sites shown in electron micrograph of Fig. 6d. (b) The presentation of a model for the location of the altered secondary structure of PM2 DNA. This model enumerates and places the location of the structures relative to each other.*

The evidence presented in this manuscript is of twofold importance. It shows that denaturation mapping can be used to locate defects when they can serve as induction sites in the duplex structure of a DNA molecule. In this study, this technique has been used to locate the induction sites in the form I molecules of the circular DNA of PM2. These sites appear to be four to six in number and located within the definite A-T stretches of the primary structure of the DNA. The success of this approach depends on the ability to perform a comparative analysis between molecules with and without structural defects.

In the case of circular DNA it is necessary to employ alignment procedures that allow for unambiguous assignment of loop positions. This is aided enormously by the asymmetry of the pattern, and we must accept that this fortuitous behavior of PM2 DNA was a considerable advantage in this study. However, with the use of a restriction enzyme in which a circular molecule can be cleaved into a unique linear, it should be possible to obtain precise alignments. This study was initiated without the knowledge or availability of a suitable restriction enzyme for PM2 DNA. However, in the case of simian virus 40 DNA, restriction enzymes have been employed to map the sites of the S1 single-stranded endonuclease (2). It would be extremely interesting to utilize the approach in this study, coupled with the appropriate restriction enzyme, to map the HCHO induction sites of SV40 DNA. These sites should map very close to the S1 sites.

The altered secondary structure found in form I circular DNA is considered to be due to a difference in the free energies when this form is compared with the form II DNA (3). The A-T bonds found in the DNA helix would take less energy to disrupt than the guanine-cytosine bonds. A stretch of A-T-rich base pairs would be the likely site of hydrogen bond disruption in any DNA helix that was under bending or torsional strain caused by supercoiling. The data showing that these induction sites are located in the A-T regions further support the localization of the altered hydrogen bonding found by the ^3H exchange data and HCHO kinetic analysis data on PM2 DNA (R. J. Jacob et al., Nucleic Acids Res., in press). It would be interesting to speculate on the role of the altered hydrogen bonding in transcription, replication, and integration of circular DNA. The possible functions for these regions are being examined in a variety of circular DNAs and will be reported when the data is complete.

ACKNOWLEDGMENTS

We would like to thank W. Hellmann for expert technical assistance with electron microscopy and F. Nehmadi for superior technical help in phage growth and DNA isolation. In addition, we are grateful to T. Beerman, A. Mazaites, M. Gutai, A. Chaudhuri, and G. Kitos for discussion or review of the manuscript. This work was supported by a Public Health Service grant from the National Cancer Institute (CA12784), and one of us (J.L.) is a recipient of a Public Health Service Career Development Award CA70514 from the National Cancer Institute.

LITERATURE CITED

1. Baev, A. S., Y. L. Lyubehenko, Y. S. Lazurkin, E. N. Trifonov, and M. D. Frank-Kamenetskii. 1972. Study of low melting segments in T_2 phage DNA by electron microscopy and kinetic formaldehyde method. Mol. Biol. **6**:760-766.
2. Beard, P., J. F. Morrow, and P. Berg. 1973. Cleavage of circular, superhelical SV40 DNA to a linear-duplex by S_1 nuclease. J. Virol. **12**:1303-1313.
3. Beerman, T. A., and J. Lebowitz. 1973. Further analysis of the altered secondary structure of superhelical DNA. Sensitivity to methylmercuric hydroxide, a chemical probe for unpaired bases. J. Mol. Biol. **79**:451-470.
4. Bricker, C. E., and H. R. Johnson. 1945. Spectrophotometric methods for determining formaldehyde. Anal. Chem. **7**:400.
5. Dean, W., and J. Lebowitz. 1971. Partial alteration of secondary structure in native superhelical DNA. Nature N. Biol. **231**:5-8.
6. Espejo, R. T., and E. S. Canelo. 1968. Properties of bacteriophage PM2: a lipid-containing bacterial virus. Virology **34**:738-747.
7. Espejo, R. T., E. S. Canelo, and R. L. Sinsheimer. 1969. DNA of bacteriophage PM2: a closed circular double-stranded molecule. Proc. Nat. Acad. Sci. U.S.A. **63**:1164-1168.
8. Feldman, M. Y. 1967. Reaction of formaldehyde with nucleotides and ribonucleic acid. Biochim. Biophys. Acta **155**:305-327.
9. Gordon, C. N., and A. K. Kleinschmidt. 1968. High contrast staining of individual nucleic acid molecules. Biochim. Biophys. Acta **155**:305-307.
10. Inman, R. B. 1966. A denaturation map of the λ phage DNA molecule determined by electron microscopy. J. Mol. Biol. **18**:464-476.
11. Inman, R. B. 1967. Denaturation maps of the left and right sides of the lambda DNA molecules determined by electron microscopy. J. Mol. Biol. **28**:103-116.
12. Inman, R. B., and M. Schnos. 1970. Partial denaturation of thymine and 5-bromouracil containing λ DNA in alkali. J. Mol. Biol. **49**:93-98.
13. Kato, A. C., K. Bartok, M. J. Fraser, and D. T. Denhart. 1973. Sensitivity of superhelical DNA to a single-strand specific endonuclease. Biochim. Biophys. Acta **308**:68-78.
14. Kleinschmidt, A. K. 1968. Monolayer techniques in electron microscopy of nucleic acid molecules, p. 361. *In* L. Grossman and K. Moldave (ed.), Methods in enzymology, vol. 12B. Academic Press Inc., New York.
15. Lazurkin, Y. S., M. D. Frank-Kamenetskii, and E. N. Trifonov. 1970. Melting of DNA: its study and application as a research method. Biopolymers **9**:1253.
16. Printz, M., and P. H. Von Hippel. 1965. Hydrogen exchange studies of DNA structure. Proc. Nat. Acad. Sci. U.S.A. **53**:363-370.